Int. J. Electrochem. Sci., 10 **(2015)** 7493 - 7504

International Journal of
ELECTROCHEMICAL
SCIENCE
www.electrochemsci.org

Corrosion Behavior of API 2H and API 4F Steels in Freely Aerated 4.0 % Sodium Chloride Solutions

El-Sayed M. Sherif[1,2,*] *and Magdy M. El Rayes*[3,4]

[1] Center of Excellence for Research in Engineering Materials (CEREM), Advanced Manufacturing Institute (AMI), King Saud University, P. O. Box 800, Al-Riyadh 11421, Saudi Arabia
[2] Electrochemistry and Corrosion Laboratory, Department of Physical Chemistry, National Research Centre (NRC), Dokki, 12622 Cairo, Egypt
[3] Department of Mechanical Engineering, College of Engineering, King Saud University, P.O. Box 800, Al-Riyadh 11421, Saudi Arabia
[4] Production Engineering Department, Faculty of Engineering, Alexandria University, Egypt.
[*]E-mail: esherif@ksu.edu.sa; emsherif@gmail.com

Received: 8 June 2015 / *Accepted:* 2 July 2015 / *Published:* 28 July 2015

The corrosion behavior of API 2H grade 50 and API 4F steels after 1 h and 24 h of their exposure in freely aerated stagnant 4.0 wt.% NaCl solution was reported. This study was conducted using various electrochemical and microscopic investigations including cyclic polarization, chronoamperometric current-time at an active anodic potential (–0.45 V vs. Ag/AgCl) and the nontraditional impedance spectroscopy tests. It was found that the API 2H and API 4F steels suffer both general and pitting corrosion in the employed chloride solution. Prolonging the exposure time from 1 h to 24 h of the electrodes immersion decreased the pitting corrosion for the investigated steels. The surface morphology performed using scanning electron microscopy indicated that both 2H and 4F steels develop a thick layer of the corrosion product that is responsible for decreasing their dissolution with increasing time. Results obtained from the different techniques were in good agreement with each other and confirmed clearly that the corrosion resistance of the API 2H steel is slightly better than the API 4F steel and this fact increased with prolonging the immersion time of the steels in the electrolytic chloride solution before the measurements were carried out.

Keywords: API pipeline steel; Chronoamperometry; Corrosion; Cyclic polarization; EIS

1. INTRODUCTION

Steel and its alloys are widely used materials in many applications in industry. This is because of their excellent mechanical properties and good corrosion resistance. API steels are especial category

of the most useful materials thanks to its excellent weldability, good toughness, low ductile to brittle transition temperature, high strength, and low crack sensitivity coefficient [1-5]. The API steels are being potentially used in off-shore rigs, transportation pipelines, pumps, construction and metal processing equipment, agitators, chemical processing, and in oil and gas storage tanks, etc [3-11]. With all these application, the API steels are prone to severe corrosion because of their varied exposure to harsh and aggressive media. The corrosion of these steels occurs mostly as a result of the dissolution of iron that exists as the main metal in the lattice of the API steel [3,4,12,13].

It has been reported [14-17] that the failure of steel pipelines occurs mostly due to the combined effect of the uniform corrosion and localized attack. The localized corrosion takes place in the form of pitting or galvanic corrosion at the area of welds, which results in the degradation of the pipelines [8,17]. This degradation could in most cases cause spillage of products transported through the pipeline and that may lead to an environmental catastrophe. Moreover, the pipelines may suffer severe internal corrosion under the effect of the corrosive attack of the species such as hydrogen sulphides, carbon dioxide, organic acids and salts presented in the water content accompanied with the process of oil production [14,15]. Another factor that increases the corrosion of pipelines is the alteration of microstructure, which results from the welding segments of carbon steel pipes during its manufacturing [18]. The variation of the microstructure is in turn accompanied by localized change in the phases as well as composition of the pipeline materials leading to the occurrence of galvanic corrosion by the increased dissimilarity of the base/weld metal combination [8,18].

Nemours researchers have investigated the corrosion and corrosion mitigation of pipeline steels in various harsh media [14-25]. In author's previous investigations [6,12,13,23], the corrosion of iron and API X-65 pipeline steel in sodium chloride solutions was investigated and found that iron is more prone to corrosion compared to X-65 steel. In other studies [1,3], the effect of exposure periods on the corrosion resistance of the API X-70 steel in sodium chloride solutions and Arabian Gulf seawater was reported. It was found that by prolonging the immersion time, the uniform corrosion of X-70 decreases due to the reduction of corrosion rate as a result of corrosion product formation and its thickening with time. Moreover, the corrosion of pipeline steel X-70 and X-65 in acidic pickling solution was also investigated [8,26].

The aim of the current investigation was to report the corrosion of the API 2H and API 4F pipeline steels after their exposure for 1 h and 24 h in freely aerated stagnant 4.0 wt.% NaCl solutions. The work was performed using various electrochemical techniques, namely cyclic potentiodynamic polarization, current-time at constant anodic voltage value and impedance spectroscopy measurements. The surface morphology of the corroded API 2H and 4F steels was carried out using scanning electron microscopy investigations.

2. EXPERIMENTAL PROCEDURES

2.1. Materials and electrochemical cell

The materials investigated were API 2H grade 50 and API 4F steels having the chemical compositions in wt.% which is presented in Table 1. Sodium chloride (NaCl, 99%) was purchased

from Merck, Riyadh; Saudi Arabia and was used in the as-received condition. A conventional tri-electrode configuration electrochemical cell was applied for performing the electrochemical measurements; the API steel rod, a platinum sheet, and a Metrohm silver/ silver chloride electrode were used as a working, counter, and reference electrodes, respectively. The 2H and 4F API steel electrodes were ground with SiC emery papers up to 1000 grits for improving surface roughness. The ground steels were washed in distilled water, cleaned using acetone, washed in distilled water again and dried in air [12,13].

Table 1. Chemical composition in wt. % of tested API steel materials

Material	C	Si	Mn	P	S
API 2H steel	0.145	0.324	1.43	0.0005	0.0023
API 4F steel	0.176	0.54	1.65	0.0089	0.0079

2.2. Electrochemical measurement techniques

Electrochemical tests were obtained via the use of an Autolab Potentiostat-Galvanostat Ecochemie PGSTAT 30 after immersion periods of 1 and 24 h of the steel electrodes in 4% NaCl solution. The cyclic polarization data were collected by scanning the potential of steel from -1.2 to 0.0 V at a scan rate of 1.67 mV/s [12,13]. Chronoamperometry measurements were performed through stepping an amount of -0.450 mV for 60 min. The impedance (EIS) plots were acquired at the open circuit potential (E_{OCP}) as previously reported in the earlier studies [1,3,12,13]. All measurements were carried out in freely aerated stagnant NaCl solutions at room temperature.

2.3. Scanning electron microscopy (SEM) characterization

The surface morphology of the API 2H and 4F steel after their immersion in 4% NaCl solutions for 24 h was analyzed using a scanning electron microscope, JEOL model JSM-6610LV (Japan).

3. RESULS AND DISCUSSION

3.1. Cyclic potentiodynamic polarization (CPP) experiments

CPP experiments were carried out to study to identify the occurrence of pitting and/or uniform corrosion for the steels after being immersed in 4% NaCl solutions for 1 and 24 h. Fig. 1 shows the polarization curves obtained for the API (a) 2H and (b) 4F steel after 1 h immersion in 4.0% NaCl solutions. Similar measurements were carried out for the steels after 24 h immersion in the chloride test solution and the curves are shown in Fig. 2. Corrosion parameters namely; cathodic (β_c) and anodic (β_a) Tafel slopes, corrosion potential (E_{Corr}), corrosion current density (j_{Corr}), polarization

resistance (R_P), and corrosion rate (R_{Corr}) were obtained from Fig. 1 and Fig. 2 and recorded in Table 2. The values of steels' corrosion data were obtained as in the case of the author's earlier publications [12,13].

The curves in Fig. 1 and Fig. 2 showed that the increase of potential towards the positive direction decreases the cathodic current until the potential value reaches E_{Corr}. According to the previous work [26-28], the cathodic reaction at this condition is the oxygen reduction,

$$2H_2O + O_2 + 4e^- \rightarrow 4OH^- \quad (1)$$

While, the anodic reaction is the dissolution of iron on two steps as per these reactions [12,13],

$$Fe = Fe^{2+} + 2e^- \quad (2)$$

$$Fe^{2+} = Fe^{3+} + e^- \quad (3)$$

These iron cations are released upon the increase of potential after E_{Corr} towards the more positive direction causing higher anodic currents. The current then stays almost constant with the change of potential due to the passivation of the steel surfaces as a result of oxide film formation [12,13],

$$Fe + \frac{1}{2}O_2 + H_2O \rightarrow Fe(OH)_2 \quad (4)$$

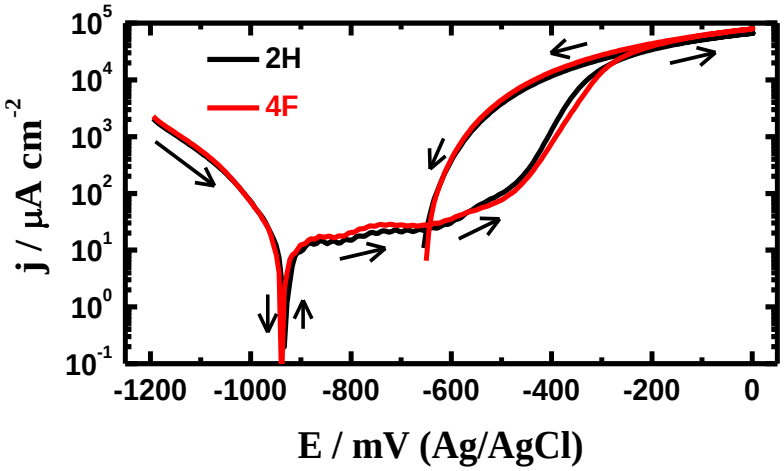

Figure 1. Cyclic potentiodynamic polarization (CPP) curves of the API (a) 2H and (b) 4F steel after being exposed in 4.0% NaCl solutions for 1 h.

In the presence of oxygen, the formed iron hydroxide is converted to the magnetite (Fe_3O_4), which is formed on the electrode surface [13];

$$3Fe(OH)_2 + \frac{1}{2}O_2 \rightarrow Fe_3O_4 + 3H_2O \quad (5)$$

This explains the active-passive region shown in the anodic polarization curves for 2H and 4F steels in 4% NaCl solutions. Up on the increase of potential towards the less negative values, a sudden increase in the values of current occurs due to the breakdown of the formed oxide layers of magnetite,

which in turn results in pitting corrosion taking place. Scanning the potential in the backward direction and the appearance of a large hysteresis loop also confirmed the presence of pits. This loop appears because of the higher values of the recorded current in the back potential scan than those obtained in its forward direction [12]. At this condition, the chloride ions attack the surface of the steel and lead to the formation of a porous film of iron chlorides (*as seen from Eq. 6 and Eq. 7*) on the surface of steel then dissolve in the solution [13]. The formation of this film allows the continuous dissolution of the steel via the increase of current in the forward direction and the occurrence of pitting corrosion.

$$Fe + 2Cl^- = FeCl_2 + 2e^- \quad (6)$$

$$FeCl_2 + Cl^- = FeCl_3 + e^- \quad (7)$$

It is seen from Fig. 1 that the corrosion behavior of 2H and 4F steels in the chloride solution is almost similar except that the dissolution of 4F is slightly higher. This was further indicated by the values of corrosion parameters presented in Table 2. Where, the values of j_{Corr} and R_{Corr} were higher and also the value of R_P was smaller in case of 4F steel compared to 2H one.

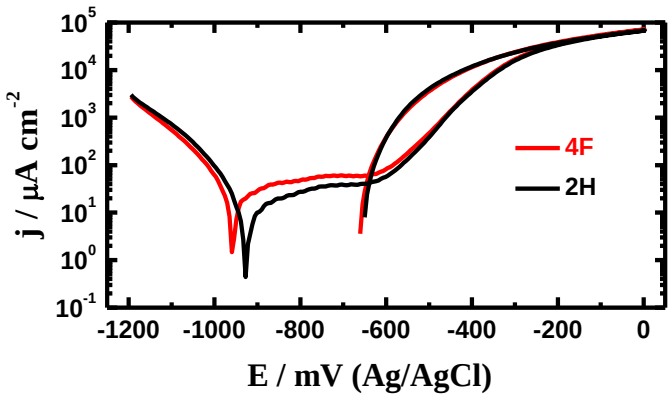

Figure 2. The CPP curves of the API (a) 2H and (b) 4F steel after 24 h immersion in 4.0% NaCl solutions.

Table 2. Polarization data of the API 2H and 4F steel in 4% NaCl solutions.

API Steel	Corrosion parameter					
	β_c /Vdec^{-1}	E_{Corr} /V	β_a /Vdec^{-1}	j_{Corr} /μA cm^{-2}	R_p /Ω cm^2	R_{Cor}/ mpy
2H (1 h)	0.08	–0.928	0.128	10	2.14	0.116
4F (1 h)	0.075	–0.932	0.140	12	1.77	0.140
2H (24 h)	0.09	–0.912	0.100	8.5	2.42	0.099
4F (24 h)	0.085	–0.945	0.095	17	1.15	0.198

Prolonging the exposure time of the steels in the sodium chloride solution to 24 h (Fig. 2) led to decreasing the uniform corrosion of 2H but on the other side increased the uniform corrosion of 4F steel. This because the CPP curve for the API 4F steel recorded higher cathodic and anodic currents as

well as higher values of j_{Corr} and R_{Corr} and lower R_P value compared to the values obtained for 2H steel either after 1 h or 24 h immersion in the solution of 4% NaCl. As for the pitting corrosion, it is clear that the area of the hysteresis loops recorded in Fig. 2 are smaller compared to the same loops shown in Fig. 1, which indicate that the pitting corrosion of both 2H and 4F steels decreases with the increase of the exposure time from 1 h to 24 h immersion. The CPP data thus confirm that the investigated API 2H steel has slightly better corrosion resistance than the 4F steel in the near neutral test chloride solutions.

3.2. Chronoamperometric measurements and SEM investigations

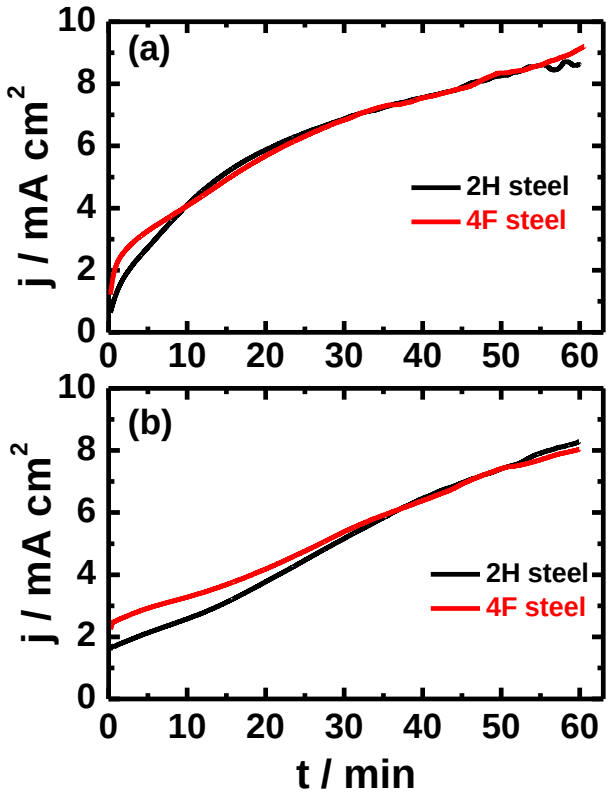

Figure 3. Chronoamperometric curves obtained for the API 2H and 4F steel after 1 h (a) and (b) 24 h immersion in 4.0% NaCl solutions followed by applying a potential of -0.45 V for 1 h.

In order to obtain a clearer view on the dissolution of the API 2H and API 4H steels and whether pitting corrosion does occur at a high anodic potential value, the chronoamperometric current-time measurements were carried out. Fig. 3 shows the chronoamperometric current-time curves obtained for the API 2H and API 4F steels after (a) 1 h and (b) 24 h immersion in 4.0% NaCl solutions followed by applying a potential of –0.45 V vs. Ag/AgCl for 1 h. It is seen from Fig. 3(a) that the current increases from the first moment of applying the anodic active potential and continue increasing with time for both 2H and 4F steels immersed for 1 h in the chloride solution. This current-time behavior proves that the investigated steels suffer uniform corrosion and severe pitting attack. The

occurrence of uniform corrosion was indicated by the high values of the measured current, while pitting attack was revealed by the continuous increase of the current values with elongating the time of the applied anodic potential value. It is also seen from Fig. 3 that the current-time behavior of the API 2H and API 4F steels is almost the same indicating that these steels corrode similarly in 4% NaCl solutions.

Prolonging the immersion time to 24 h before measurement, Fig. 3(b), slowed down the fast increase of current with time, particularly in the first 10 min of the anodic potential application. This is due to the thickening of the formed oxides on steels during their immersion for 24 h before applying the constant potential value, –0.45 V, and before measuring the current vs. time. Also, the API 2H steel shows lower current values in the first 30 min. compared to 4F steel. Further increasing the time of the applied potential increased the current values and led to the pitting attack. Here, chloride ions from the solution penetrate the oxide and attack the surface of the steels causing its dissolution as indicated by Eq. (6) and Eq. (7). The chronoamperometric current-time curves for the API steels are in good agreement with the results obtained from the CPP curves indicating that the investigated API steels suffer both uniform and pitting corrosion in 4% NaCl solutions.

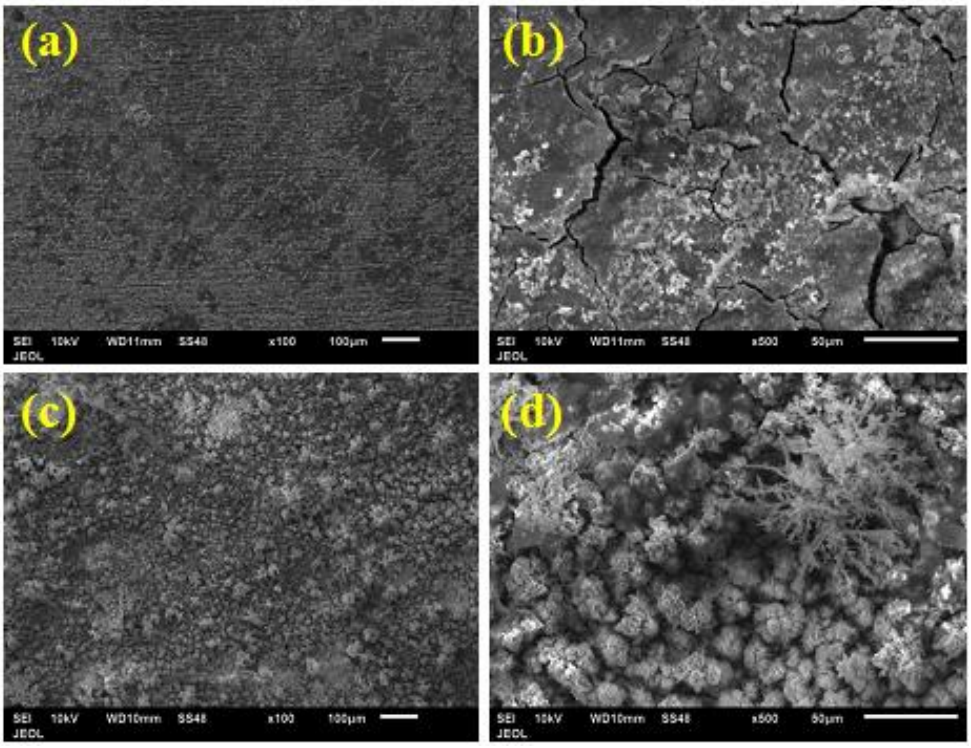

Figure 4. Scanning electron microscopy images obtained from the surface of the API; (a) & (b) 2H steel and (c) & (d) 4F steel, after 24 h immersion in NaCl solutions then applying a potential of -0.45 V for 1 h.

In order to investigate the surface morphology of the corroded 2H and 4F steels, SEM images were obtained. The SEM micrographs obtained from the surface of the API steels; (a) & (b) 2H steel and (c) & (d) 4F steel, after 24 h immersion in 4.0% NaCl solutions followed by applying a potential of -0.45 V vs. Ag/AgCl for 1 h. It is noted from Fig. 4, image (a) that the majority of the surface is

covered with bright corrosion products and some areas appear darker and may have pits due to the application of the active anodic potential and the corrosiveness action of the chloride ions. Elongating an area that contains corrosion products *(as can be seen from Fig. 4b)* indicated that the layer is thick and cracked, which means it may have pits underneath. On the other hand, the images taken for the API 4F steel surface depicted that almost all the surface had thick and bright corrosion product layers (Fig. 4c). Extending an area of the surface (Fig. 4(d)) showed that the corrosion product layers had shaped like flowers that are different from those obtained for the API 2H steel at the same condition. However, the pitting corrosion behavior obtained from the chronoamperometric current-time curves is shown in Fig. 3(b) which indicates that the pits are hidden below the thick oxide films.

3.3. Electrochemical impedance spectroscopy (EIS) measurements

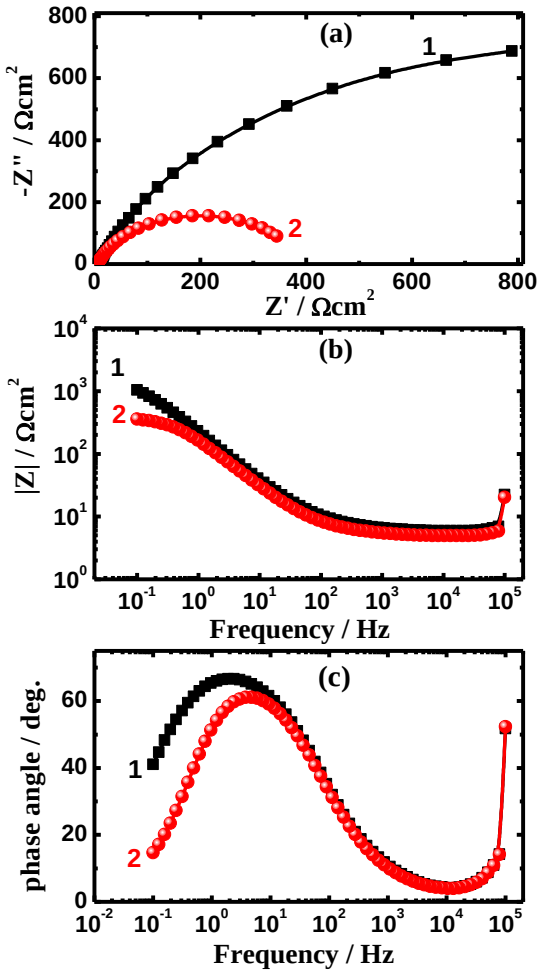

Figure 5. Typical (a) Nyquist, (b) Bode impedance and (c) Bode phase angle plots of the API (1) 2H and (2) 4F steel immersed in 4.0% NaCl solutions for 1 h.

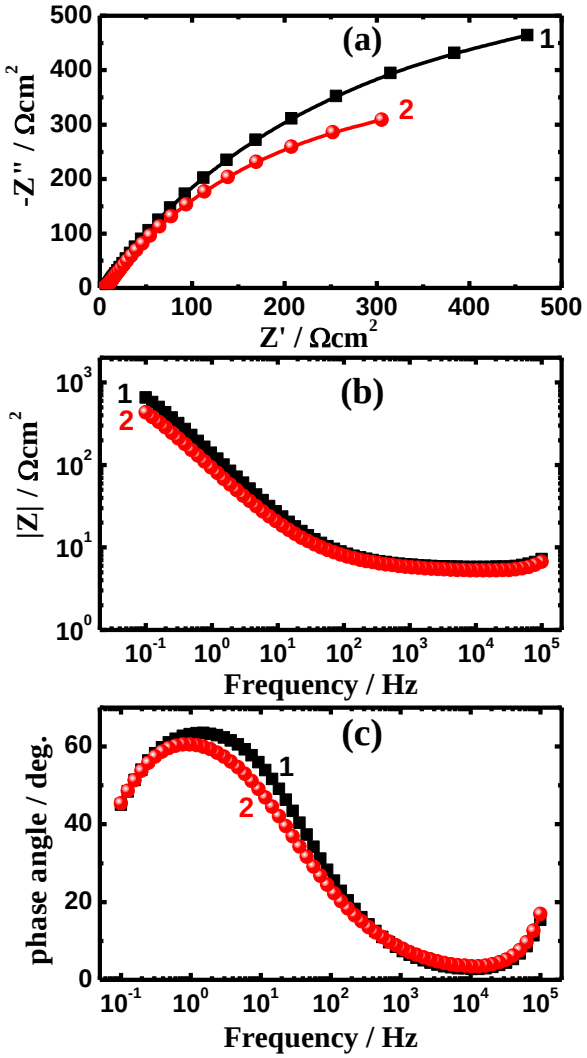

Figure 6. Typical (a) Nyquist, (b) Bode impedance and (c) Bode phase angle plots of the API (1) 2H and (2) 4F steel after 24 h immersion in 4.0% NaCl solutions.

EIS has been employed frequently in determining the metals' and alloys' kinetics for electron transfer reactions at the metal/solution interface [1,3,12,13,26-29]. Fig. 5 shows (a) Nyquist, (b) Bode impedance and (c) Bode phase angle plots obtained for the API (1) 2H and (2) 4F steel immersed in 4.0% NaCl solutions for 1 h. The Nyquist, Bode impedance of the interface and the Bode phase angle were also obtained for the API steels after 24 h immersion in NaCl solutions and the plots are shown respectively in Fig. 6. The obtained EIS data were best fitted to the equivalent circuit model displayed in Fig. 7 and the obtained values from this circuit are presented in Table 2. The elements of the depicted circuit can be defined as; R_s is the solution resistance, Q represents the constant phase elements (CPEs), R_{P1} is the polarization resistance between the surface of the API steel and the oxide film that was formed during the immersion of the electrode in the chloride for the meant exposure periods before measurement (1 h and 24 h), C_{dl} represents a double layer capacitor, and R_{P2} is another rout of the polarization resistance and represents the corrosion resistance between the formed corrosion product layer and the solution interface [29].

It is obvious from Fig. 5(a) for the steels after 1 h immersion in the chloride test solution that the API 2H steel showed a bigger semicircle diameter than that obtained for the API 4F steel, which indicates that the corrosion resistance is higher for the API 2H steel. The change of the impedance of the interface (|Z|, Fig. 5(b)) as well as the degree of phase angle (ϕ, Fig. 5(c)) with frequency indicated clearly that the API 2H steel had higher |Z| and the maximum values of ϕ compared to the values obtained for the API 4H steel [26-29]. This confirms that 2H steel had better corrosion resistance than 4F steel after short immersion period in NaCl solutions, 1 h. This is also seen from the listed parameters in Table 2, where the resistance values of R_S, R_{P1} and R_{P2} are higher for the 2H steel. Also, the CPE (Q) with its n value a little higher than 0.70 express a double layer capacitor having few pores like it appeared by the SEM images (Fig. 4) [30].

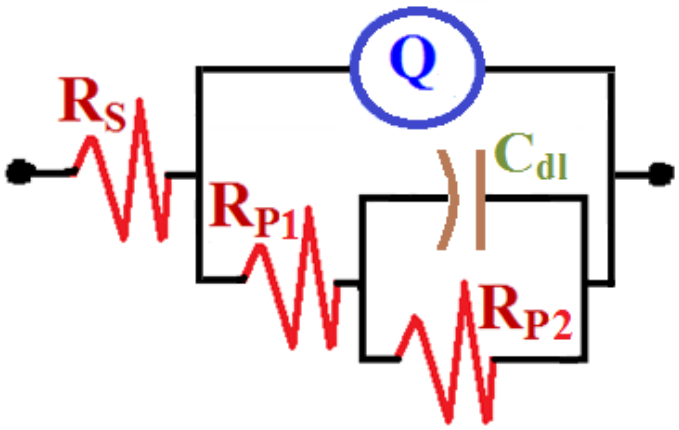

Figure 7. Equivalent circuit that fits our EIS data.

Increasing the exposure time to 24 h for the immersion of the API 2H and API 4F ~~pipeline~~ steels almost gives the same impedance plots, Fig. 6. It is seen that the diameter of the Nyquist semicircle, |Z|, and ϕ were higher for the API 2H steel than the API 4F steel. This was also reflected on the obtained values of resistances, Q, C_{dl} listed in Table 3 and whose were in the favor of the higher resistance against corrosion for the API 2H compared to 4F steel. The EIS results thus confirm the obtained results from CPP curves, chronoamperometry and the surface morphology investigations.

Table 3. Parameters obtained from EIS plots for the API 2H and 4F steels after different immersion periods in 4% NaCl solutions.

Sample	Parameters					
	R_S/ Ω cm^2	Q		R_{P1}/ Ω cm^2	C_{dl}/ F cm^{-2}	R_{P2}/ Ω cm^2
		Y_Q/ F cm^{-2}	n			
API 2H steel (1 h)	8.46	0.000729	0.72	64.06	0.0001726	696
API 4F steel (1 h)	7.35	0.001011	0.71	37.19	0.000264	388
API 2H steel (24 h)	6.46	0.001655	0.76	48.13	0.000841	411
API 4F steel (24 h)	5.75	0.002920	0.72	26.84	0.000597	277

4. CONCLUSIONS

The corrosion behavior of two different API steels, namely 2H and 4F, in 4% NaCl solutions was reported and the outcome is summarized as following:

1. CPP curves obtained for the steels immersed for 1 h and 24 h in NaCl solutions indicated that these steels suffer general and pitting corrosion and the later was reduced with prolonging the immersion time due to the oxide film formatting and thickening.
2. Current time curves obtained at –0.45 V confirmed the polarization data that the investigated API steels corrode via their uniform and pitting attacks as indicated by the obtained high values of current and its continuous increases with time.
3. SEM micrographs displayed that the surfaces had thick layer of iron oxides, which led to decreasing the dissolution of the steels, particularly at long immersion time, 24 h.
4. The results obtained from Nyquist and Bode plots collected for both steels agreed with CPP and chronoamperometric data that the API 2H steel has slightly better corrosion resistance when compared to the 4F steel one, whether those steels were immersed in 4% NaCl solution for 1 h or 24 h and the increase of exposure time lessens the corrosivity of NaCl on the examined API steels.

ACKNOWLEDGEMENT
This project was funded by the National Plan for Science, Technology and Innovation (MARRIFAH), King Abdulaziz City for Science and Technology, Kingdom of Saudi Arabia, Award Number (11-ADV1033-02).

References

1. El-Sayed M. Sherif, Abdulhakim A. Almajid, *J. Chem.*, 2014 (2014) 7.
2. Mostafa Alizadeh and Sajjad Bordbar , *Corros. Sci.*, 70 (2013) 170.
3. El-Sayed M. Sherif, Abdulhakim A. Almajid, *Int. J. Electrochem. Sci.*, 10 (2015) 34.
4. A. Yakubtsov, P. Poruks and J. D. Boyd, *Mater. Sci. Eng. A*, 480 (2008) 109.
5. A. Guenbour, M. A. Hajji, E. M. Jallouli and A. Ben Bachir, *Appl. Surf. Sci.*, 253 (2006) 2362.
6. El-Sayed M. Sherif, Abdulhakim A. Almajid, Khalil Abdelrazek Khalil, Harri Junaedi and F. H. Latief, *Int. J. Electrochem. Sci.* 8 (2013) 9360.
7. M. C. Zhao, K. Yang and Y. Y. Shan, *Mater. Lett.*, 57 (2003) 1496.
8. El-Sayed M. Sherif, Asiful H. Seikh, *Int. J. Electrochem. Sci.*, 10 (2015) 209.
9. M. A. Hegazy, H. M. Ahmed and A. S. El-Tabei, *Corros. Sci.*, 53 (2011) 671.
10. A. Hernández-Espejel and M. A. Domínguez-Crespo, *Corros. Sci.*, 53 (2010) 2258.
11. A. Bellaouchou, B. Kabkab, A. Guenbour and A. Ben Bachir, *Prog. Org. Coat.*, 41 (2001) 127.
12. El-Sayed M. Sherif, R.M. Erasmus, and J.D. Comins, *Electrochim. Acta*, 55 (2010) 3657.
13. El-Sayed M. Sherif, *Mater. Chem. Phy.*, 129 (2011) 961.
14. X. Jiang, Y.G. Zheng, W. Ke, *Corros. Sci.*, 47 (2005) 2636.
15. D. Hardie, E. A. Charles and A. H. Lopez, *Corros. Sci.*, 48 (2006) 4378.
16. C.T. Kwok, S.L. Fong, F.T. Cheng and H.C. Man, *J. Mater. Proc. Technol.*, 176 (2006) 168.
17. F.Y. Ma and W.H. Wang, *Mater. Sci. Eng. A*, 430 (2006) 1.
18. T. Hemmingsten, H. Hovdan, P. Sanni, and N.O.Aagotnes, *Electrochim. Acta*, 47(2002) 3949.
19. S. Nešić, *Corros. Sci.*, 49 (2007) 4308.
20. M.A. Migahed, *Prog. Org. Coat.*, 54 (2005) 91.
21. M.A. Hegazy, H.M. Ahmed and A.S. El-Tabei, *Corros. Sci.*, 53 (2011) 671.

22. S. Junaedi, A.A. Al-Amiery, A. Kadihum, A.A.H. Kadhum and A.B. Mohamad, *Int. J. Mol. Sci.*, 14 (2013) 11915.
23. El-Sayed M. Sherif, *Molecules*, 19 (2014) 9962.
24. E.S. Meresht, T.S. Farahani and J. Neshati, *Corros. Sci.*, 54 (2012) 36.
25. B.R. Tian and Y.F. Cheng, *Corros. Sci.*, 50 (2008) 773.
26. Asiful H. Seikh and El-Sayed M. Sherif, *Int. J. Electrochem. Sci.*, 10 (2015) 895.
27. El-Sayed M. Sherif, *Int. J. Electrochem. Sci.*, 6 (2011) 2284.
28. El-Sayed M. Sherif, *Int. J. Electrochem. Sci.*, 6 (2011) 3077.
29. El-Sayed M. Sherif, H.S. Abdo and A.A. Almajid, *Materials*, 8 (2015) 2127.
30. Zhe Zhang , Shenhao Chen, Yanhui Li, Shuhuan Li, Liang Wanga, *Corros. Sci.*, 51 (2009) 291.